**ARTICLE** - Platelet Biology & its Disorders

# Differentiating pathogenic from bystander autoantibodies in immune thrombocytopenia using intact glycoprotein-deficient megakaryocytes

Nanyan Zhang,[1] Günalp Uzun,[2] Tamam Bakchoul,[2] Brian R. Curtis[1] and Peter J. Newman[1,3,4]

[1]Versiti Blood Research Institute, Milwaukee, WI, USA; [2]Institute for Clinical and Experimental Transfusion Medicine, University Hospital Tübingen, Tübingen, Germany and [3]Departments of Pharmacology and [4]Cell Biology, Medical College of Wisconsin, Milwaukee, WI, USA

**Correspondence:** N. Zhang
nzhang@versiti.org

**Received:** July 29, 2025.
**Accepted:** December 5, 2025.
**Early view:** December 11, 2025.

**https://doi.org/10.3324/haematol.2025.288832**

**Title**

# Differentiating pathogenic from bystander autoantibodies in immune thrombocytopenia using intact glycoprotein-deficient megakaryocytes

**Authors**

Nanyan Zhang, Günalp Uzun, Tamam Bakchoul, Brian R. Curtis, and Peter J. Newman

## Supplemental Materials

**Supplementary Table 1**

# Table S1: ITP patient autoantibody testing results.

| | Site 1 diagnostic test | | | | | |
|---|---|---|---|---|---|---|
| | Platelet Eluates | | Plasma ACA | | Plasma WMK | |
| Patient ID | IIb-IIIa | Ib/IX | IIb-IIIa | Ib/IX | IIb-IIIa | Ib/IX |
| **Patient-1** | NT | NT | **pos** | neg | **pos** | neg |
| **Patient-2** | NT | NT | **pos** | neg | **pos** | neg |
| **Patient-3** | pos | pos | **pos** | neg | **pos** | neg |
| **Patient-4** | NT | NT | **pos** | neg | **pos** | neg |
| **Patient-5** | pos | pos | neg | neg | **pos** | neg |
| **Patient-6** | pos | pos | neg | neg | **pos** | neg |
| **Patient-7** | pos | pos | neg | neg | **pos** | neg |
| **Patient-8** | pos | pos | neg | neg | **pos** | neg |
| **Patient-9** | NT | NT | neg | **pos** | neg | **pos** |
| **Patient-10** | NT | NT | **pos** | **pos** | **pos** | **pos** |
| **Patient-17** | NT | NT | neg | **pos** | neg | neg |
| **Patient-32** | NT | NT | **pos** | neg | neg | neg |
| **Patient-33** | pos | pos | neg | neg | neg | neg |
| **Patient-34** | NT | NT | **pos** | neg | **pos** | neg |
| *Patient-35* | pos | pos | **pos** | neg | **pos** | neg |
| *Patient-36* | pos | pos | **pos** | neg | **pos** | neg |
| *Patient-37* | pos | pos | **pos** | neg | **pos** | neg |
| *Patient-38* | pos | pos | **pos** | neg | **pos** | neg |
| *Patient-39* | pos | pos | neg | neg | neg | neg |
| *Patient-40* | pos | pos | neg | neg | **pos** | neg |
| *Patient-41* | pos | pos | neg | neg | **pos** | neg |
| *Patient-42* | pos | pos | neg | **pos** | **pos** | neg |
| *Patient-43* | pos | pos | neg | **pos** | **pos** | neg |
| *Patient-44* | pos | pos | neg | **pos** | **pos** | neg |
| *Patient-45* | pos | pos | **pos** | **pos** | neg | neg |
| *Patient-46* | pos | pos | **pos** | **pos** | **pos** | neg |
| *Patient-47* | pos | pos | **pos** | **pos** | **pos** | neg |
| *Patient-48* | pos | pos | neg | **pos** | neg | neg |

PABA

ELISA

| | Site 2 diagnostic test | | | | | |
|---|---|---|---|---|---|---|
| | Platelet Eluates | | Plasma ACA | | Plasma WMK | |
| Patient ID | IIb-IIIa | Ib/IX | IIb-IIIa | Ib/IX | IIb-IIIa | Ib/IX |
| Patient-11 | pos | pos | **pos** | **pos** | neg | **pos** |
| Patient-12 | pos | pos | **pos** | **pos** | neg | **pos** |
| Patient-13 | pos | pos | neg | neg | **pos** | **pos** |
| Patient-14 | pos | pos | neg | neg | **pos** | **pos** |
| Patient-15 | pos | pos | **pos** | neg | **pos** | **pos** |
| Patient-16 | pos | pos | **pos** | neg | **pos** | **pos** |
| Patient-18 | pos | pos | **pos** | neg | **pos** | neg |
| Patient-19 | neg | pos | neg | neg | neg | neg |
| Patient-20 | pos | pos | neg | neg | neg | neg |
| Patient-21 | pos | pos | neg | neg | neg | neg |
| Patient-22 | pos | pos | **pos** | neg | **pos** | neg |
| Patient-23 | pos | pos | **pos** | neg | **pos** | neg |
| Patient-24 | pos | pos | **pos** | **pos** | **pos** | **pos** |
| Patient-25 | pos | pos | **pos** | **pos** | **pos** | **pos** |
| Patient-26 | neg | pos | neg | **pos** | **pos** | neg |
| Patient-27 | pos | pos | **pos** | **pos** | **pos** | neg |
| Patient-28 | pos | pos | **pos** | **pos** | neg | neg |
| Patient-29 | pos | pos | **pos** | **pos** | **pos** | neg |
| Patient-30 | pos | pos | **pos** | **pos** | neg | neg |
| Patient-31 | pos | pos | **pos** | **pos** | neg | neg |

MAIPA

Match

WMK$^+$/ACA$^-$

ACA$^+$/WMK$^-$

Site 1 routinely uses ELISA to detect ITP autoantibodies in patient platelet eluates and plasma. The PABA test, equivalent to the well-known MACE test and more sensitive than ELISA, is often used when patients do not have sufficient platelets to prepare eluates. The top fourteen patient plasmas from Site 1 (patient IDs highlighted in **bold**) were tested with PABA. The bottom fourteen patient plasmas (patient IDs shown in *italics*) were tested with ELISA. Site 2 uses MAIPA to detect autoantibodies in patient platelet eluates and plasma. Results from the whole megakaryocyte (WMK) assay for detecting autoantibodies in patient plasmas are presented for comparison with lab plasma ACA testing. Blue indicates cases where the WMK result matches the patient's lab ACA result. Orange indicates cases where the patient's plasma autoantibody is detectable only with WMK but not ACA. Pink indicates cases where at least one of the patient's plasma autoantibodies identified by ACA is not detected by WMK. Two cases (patient 12 and 31) from Site 2 were treated with medication to reduce antibody production, which may have rendered the antibodies undetectable by WMK; these cases were not included in the comparison. **NT** indicates samples not tested due to insufficient platelet counts. **pos** stands for positive; **neg** stands for negative.

**Table S2: gRNA sequences.**

| | Sequence from 5' to 3' |
|---|---|
| Guide 1 targeting *ITGA2B* gene | CAGCTGGAGCGACGTCATTG |
| Guide 2 targeting *ITGA2B* gene | GAGGCTGAGAAGACGCCCGT |
| Guide 1 targeting *GPIBA* gene | TCTCACAGTTGCATAACCAG |
| Guide 2 targeting *GPIBA* gene | AAAGCCCATACAACCCCCTG |
| Guide 1 targeting *GPIX* gene | CCCATGTACCTGCCGCGCCC |
| Guide 2 targeting *GPIX* gene | AGGGGTTCTGCGTCACATCG |
| Guide 1 targeting *GPV* gene | GAGGGGGACTCTACTGTGCG |
| Guide 2 targeting *GPV* gene | TCACCCCTAAGTACCGCAGG |
| T2 guide targeting AAVS1 locus | GGGGCCACTAGGGACAGGAT |

**Table S3: PCR primers for genotyping.**

| | Sequence from 5' to 3' |
|---|---|
| ITGA2B-For | CTGGGATACGCTGGAATCTG |
| ITGA2B-Rev | GCTGGCGCTTACTAAAATCA |
| GPIBA-For | ACTCCAAGAGCTCTACCTGA |
| GPIBA-Rev | GGTCCATCTAGGTGGGAATG |
| GPIX-For | CTGGTTTCCCAGAGGAGAAG |
| GPIX-Rev | GCTGAGCTGCCAGTTTATTC |
| GPV-For | ATTCTGGCGAAAGGATTGTGCC |
| GPV-Rev | GCTGCTGAGATTGCGGAAGAG |
| AAVS1-For-1 | TCGACTTCCCCTCTTCCGATG |
| AAVS1-Rev-1 | CTCAGGTTCTGGGAGAGGGTAG |
| AAVS1-Rev-2 | GGTCATTGGGCCAGGATTCTC |
| AAVS1-For-3 | CACTCGGAAGGACATATGGGAG |
| AAVS1-Rev-3 | CCTGGGATACCCCGAAGAGT |

## Supplementary Figure 1

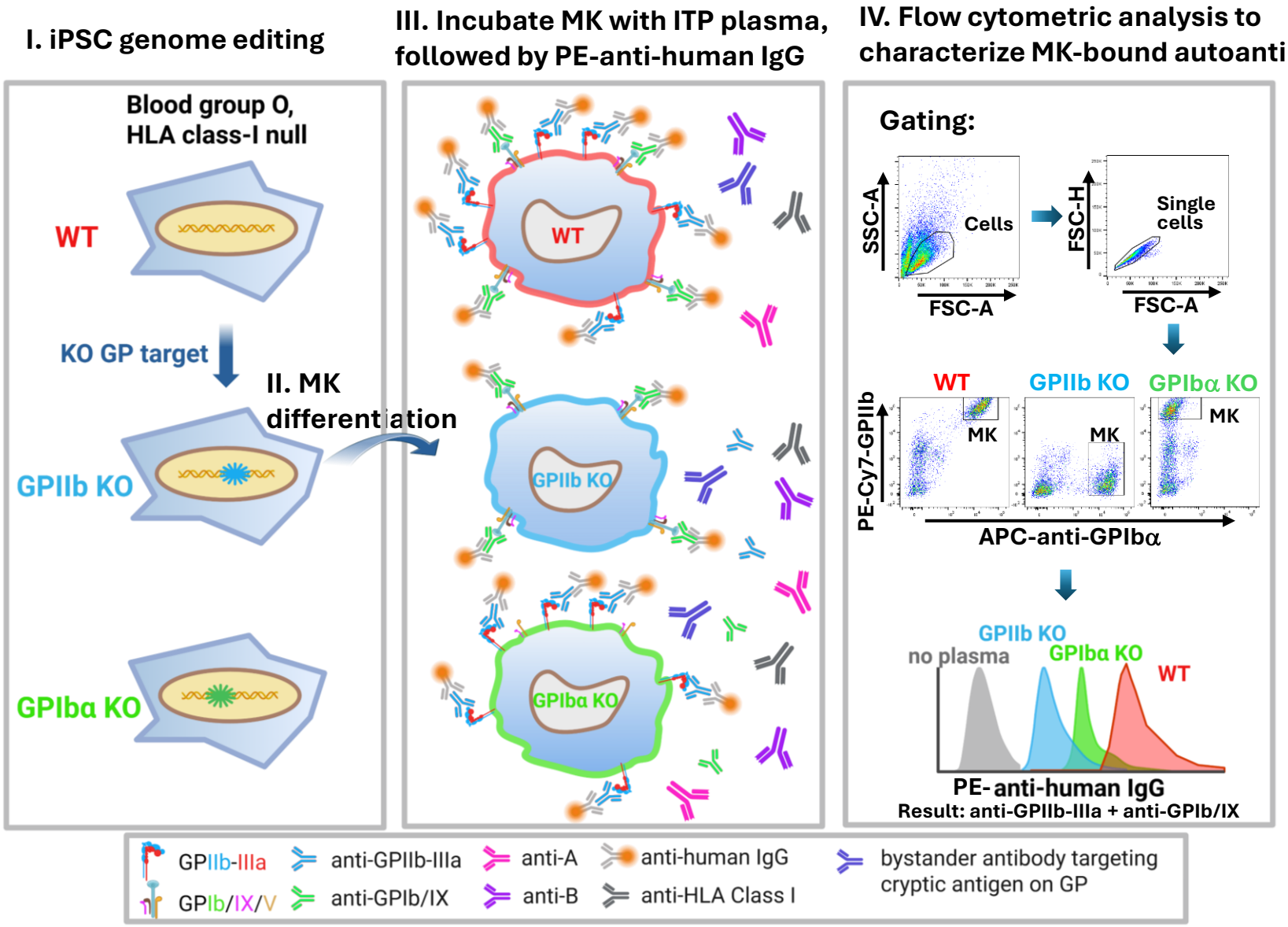


**Figure S1. Workflow for detecting plasma autoantibodies in ITP using whole megakaryocytes.** iPSC-derived MK can be cryopreserved and distributed to diagnostic laboratories for antibody testing.

# Supplementary Figure 2

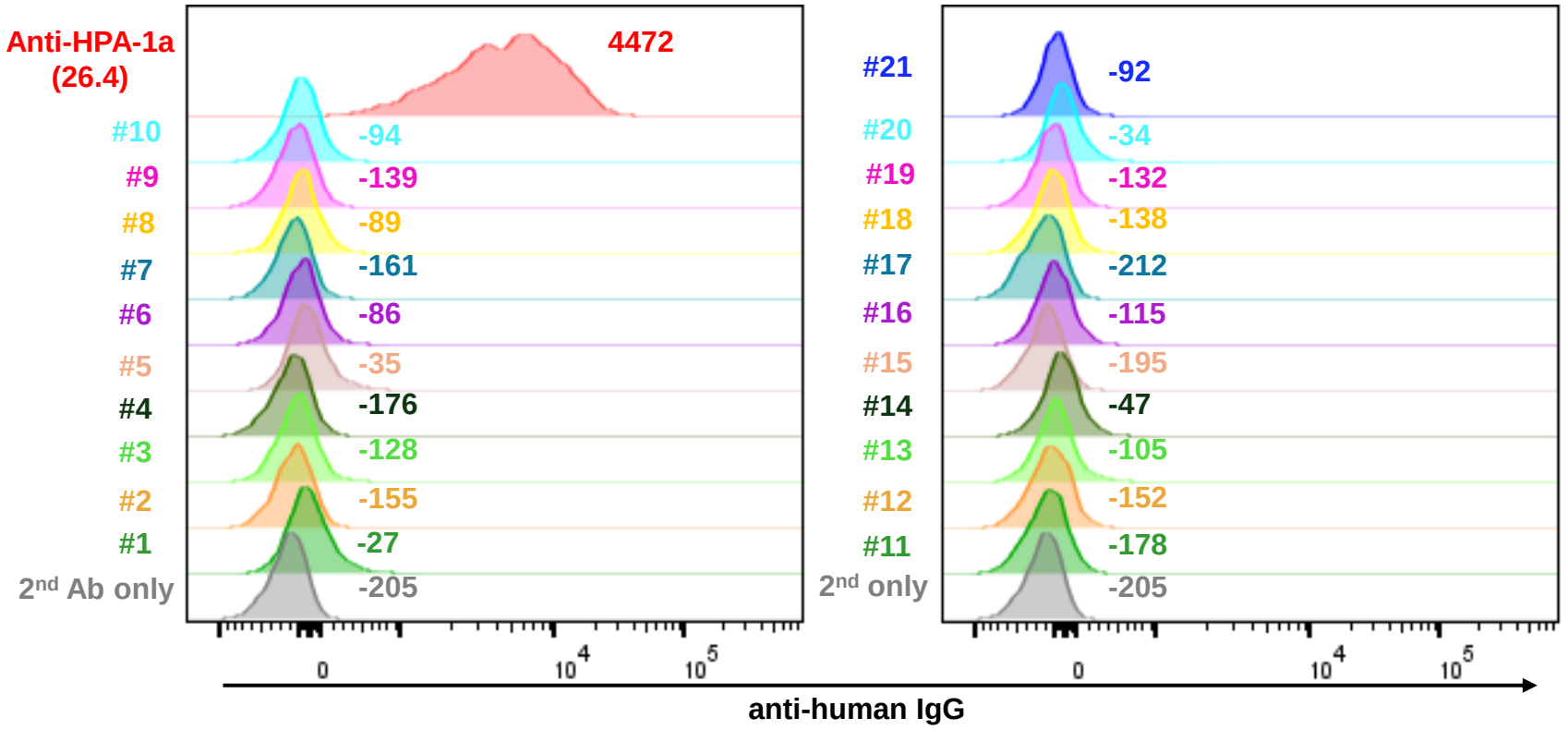


**Figure S2. Low background binding of normal human plasmas to HLA class I-negative iPSC-derived MK.** Twenty-one normal human plasma samples were tested with HLA class I-negative iPSC founder line-derived MK using flow cytometric analysis. Anti-HPA-1a (26.4) human antibody served as a positive control. MK-bound antibodies were detected with PE-conjugated donkey anti-human IgG. Color-coded numbers indicate the median fluorescence intensity of the corresponding peaks.

## Supplementary Figure 3

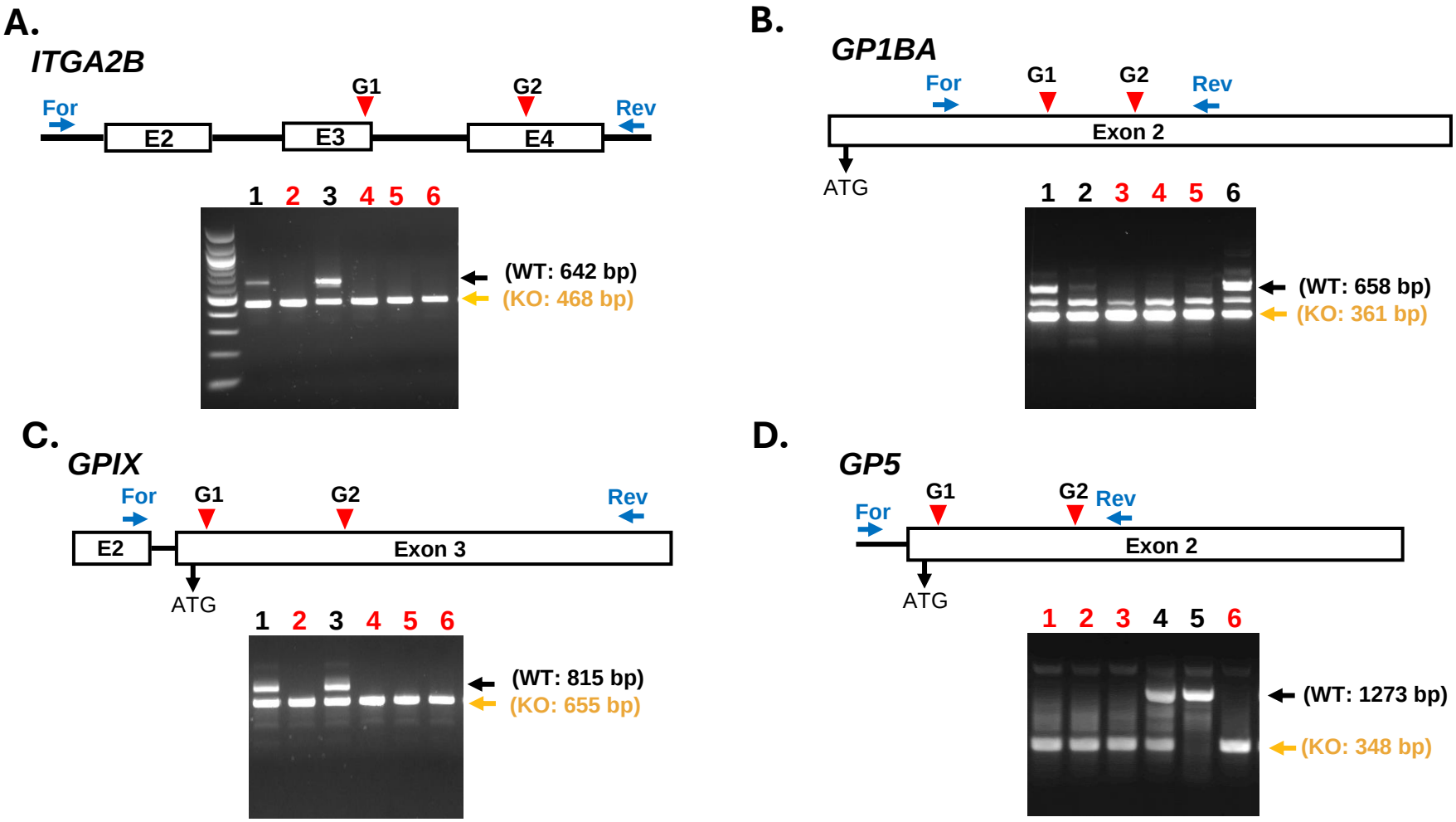


**Figure S3. Generation of glycoprotein KO iPSC clones.** Schematic representation of the *ITGA2B* (**A**), *GPIBA* (**B**), *GPIX* (**C**), and *GP5* (**D**) loci, illustrating the location of the gRNA binding sites (red arrowheads) and primer binding sites (blue arrows) for PCR genotyping. Genomic DNA from iPSC single clones, transfected with PX459 V2.0-gRNA1 and PX459 V2.0-gRNA2 targeting each respective gene, was PCR-amplified to screen for bi-allelic deletion at the targeted locus (highlighted in red). Black and orange arrows indicate the expected fragment sizes of the WT and KO alleles, respectively.

## Supplementary Figure 4

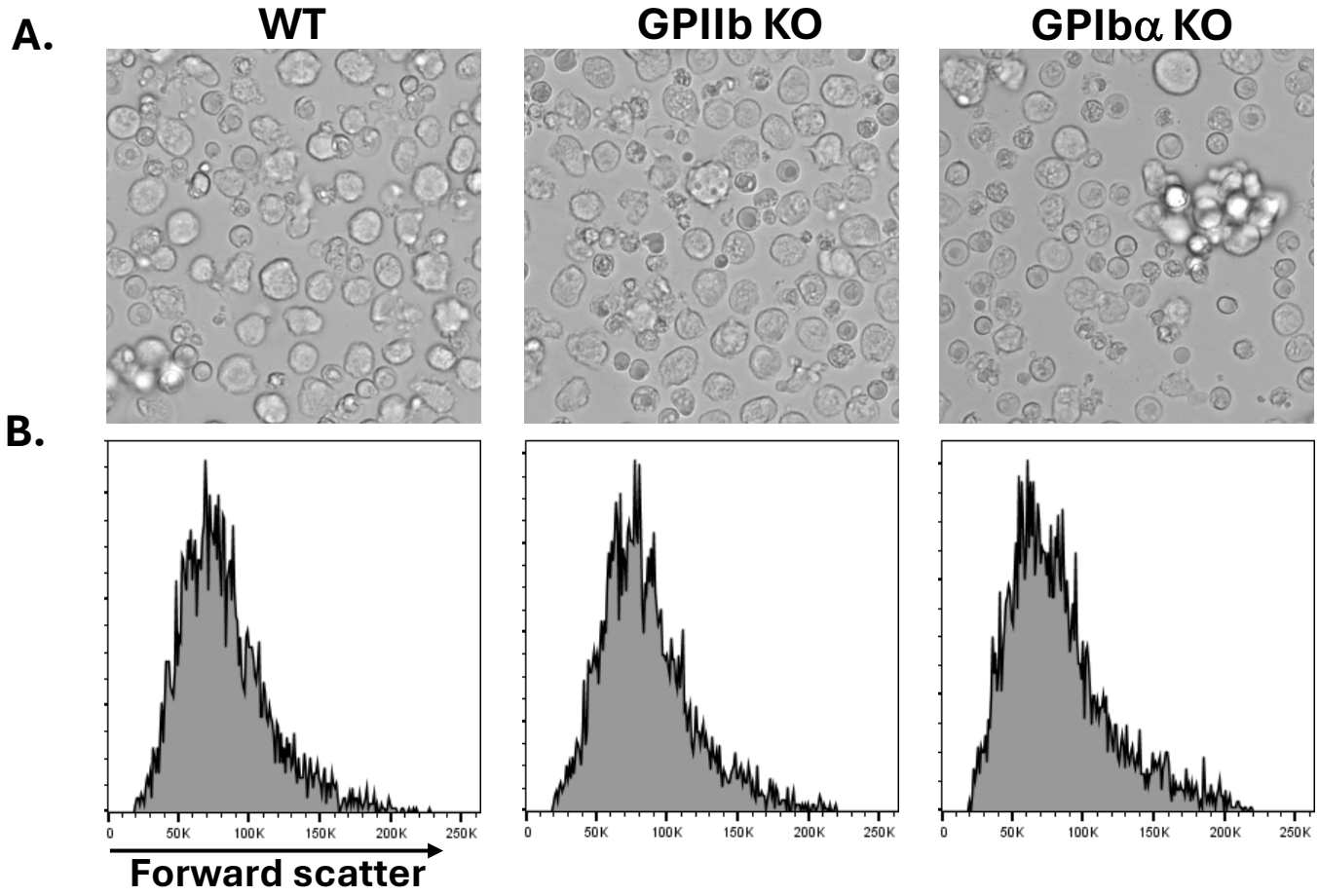


**Figure S4. Normal size distribution of glycoprotein-deficient MK. (A)** Representative images of iPSC-derived MK from various cell lines. **(B)** Flow cytometric analysis of iPSC-derived MK from different cell lines, comparing size distribution between GP KO and WT MKs.

# Supplementary Figure 5

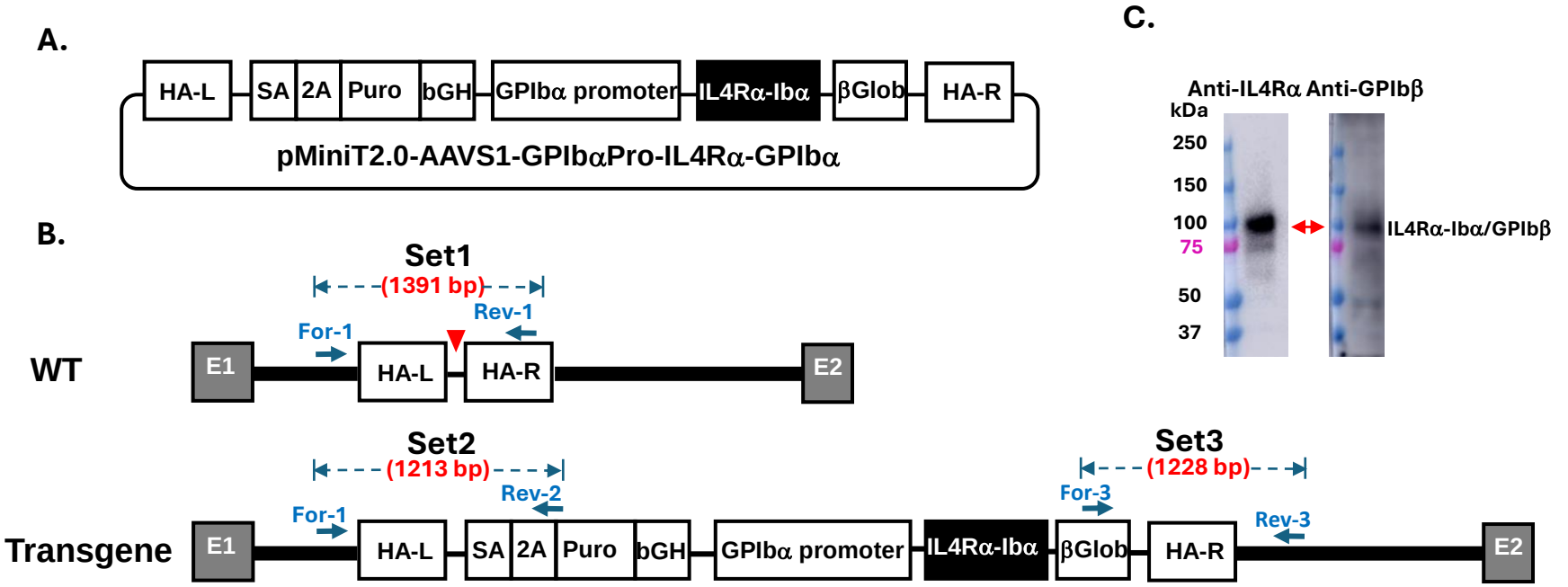


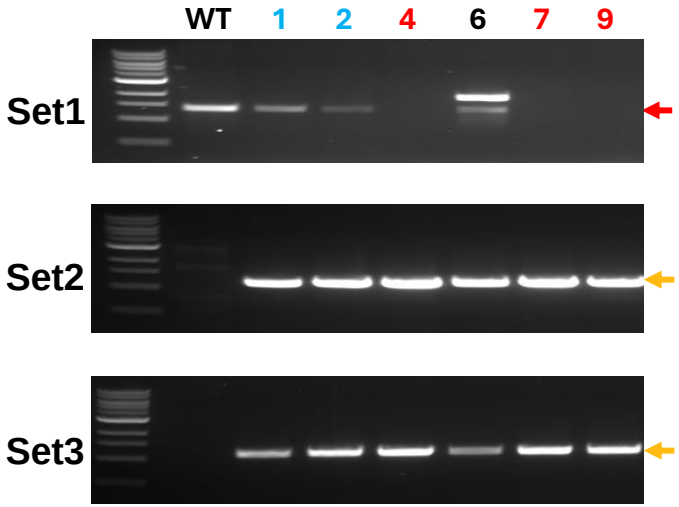


**Figure S5. Generation of IL4Rα-GPIbα iPSC clones.** (**A**) Donor plasmid targeting AAVS1 locus for IL4Rα-GPIbα expression in MKs. HA-L: left homology arm, SA: splice acceptor, 2A: T2A peptide, Puro: puromycin resistance gene, bGH: bovine growth hormone polyadenylation signal, βGlob: rabbit beta-globin polyadenylation signal, HA-R: right homology arm. (**B**) Schematic illustration of the integration site at AAVS1 locus (1st intron of *PPP2R12C*). The red arrowhead marks the T2 guide RNA binding site and blue arrows indicate primer binding sites for genotyping. Genomic DNA from iPSC single clones, transfected with PX458-T2 and AAVS1-donor plasmid, was PCR-amplified to screen for clones with transgene integration at the AAVS1 locus. Expected fragment sizes for the wild-type (WT) allele and transgene insertion are marked by red and orange arrows, respectively. Clones with single- or bi-allelic integration are labeled with blue and red numbers, respectively. **(C)** MK cell lysates from a homozygous IL4Rα-GPIbα iPSC clone were resolved by SDS-PAGE under non-reducing conditions and immunoblotted with anti-IL4Rα or anti-GPIbβ monoclonal antibodies. The red arrow indicates the complex formed by the chimeric protein and GPIbβ.

# Supplemental Figure 6

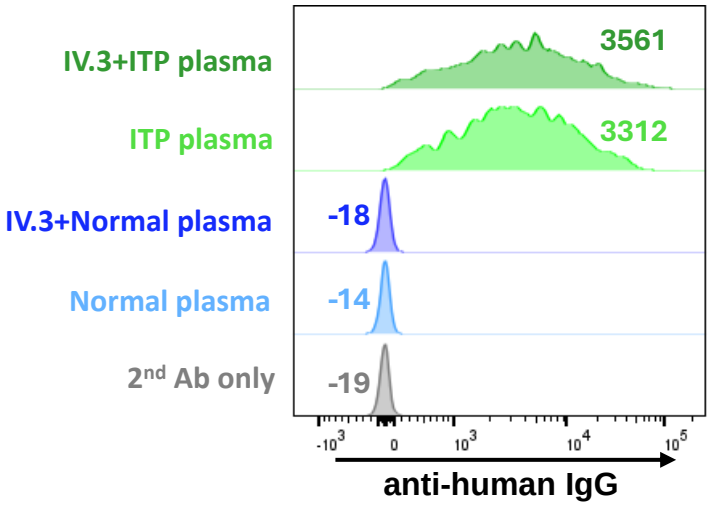


**Figure S6. Blocking FcγRIIa receptors does not affect ITP autoantibody binding to iPSC-derived MKs.** WT MKs were preincubated with 10 mg/ml anti-FcγRIIa antibody IV.3 for 20 min before being incubated with either normal human plasma or ITP plasma from Patient-2. The MK-bound autoantibodies were detected using PE-conjugated donkey anti-human IgG and analyzed by flow cytometry. Color-coded numbers indicate the median fluorescence intensity of the corresponding peaks.

## Supplemental Figure 7

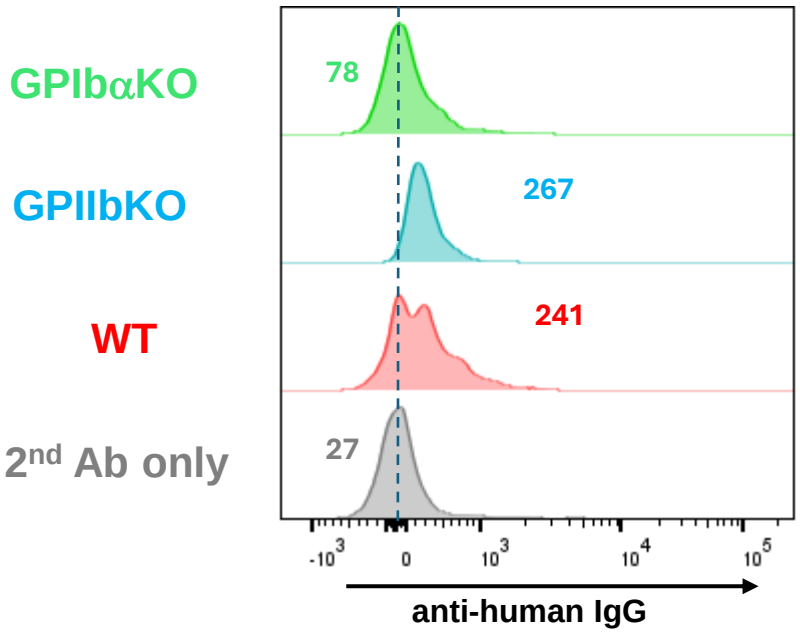


**Figure S7. Detection of a missed anti-GPIb/IX antibody in the plasma of a Bernard–Soulier syndrome (BSS) patient using WMK.** This BSS patient was suspected to harbor an anti-GPIb/IX antibody following prior blood transfusion. However, the antibody was not detected by the clinical diagnostic PABA test. In contrast, WMK successfully revealed a weak anti-GPIb/IX antibody in the patient's plasma.

## Supplementary Figure 8

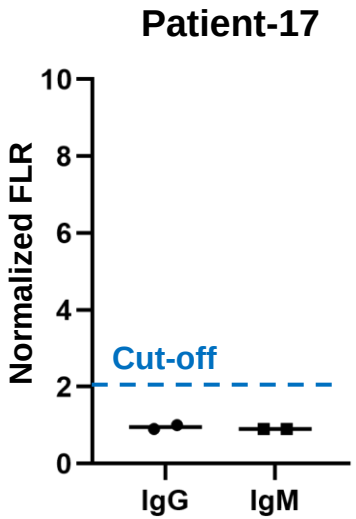


**Figure S8. Lack of detectable antibody binding to intact platelets by plasma from patient-17.** Plasma from patient-17 showed no antibody binding to human platelets from two individual donors in whole platelet flow cytometry. The cut-off for a positive in this standard clinical test is an FLR ≥ 2.0.

# Supplemental Figure 9

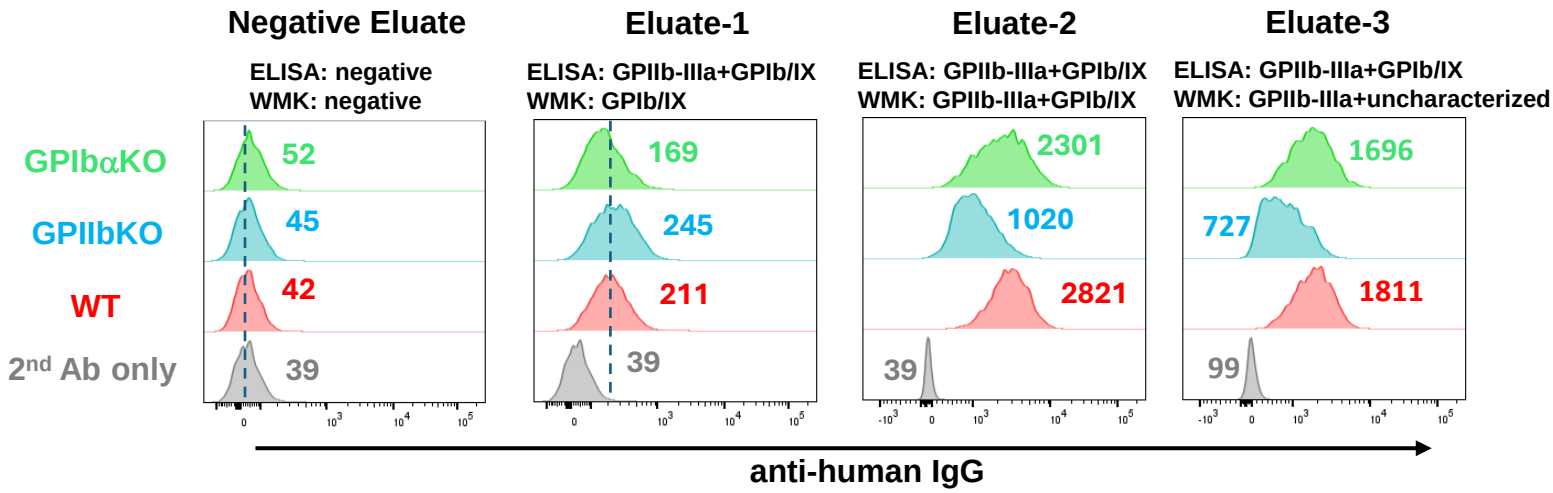


**Figure S9. Detection and characterization of ITP autoantibodies in patient platelet eluates using WMK.** Platelet eluates from three ITP patients with detectable autoantibodies in diagnostic ELISA were tested by WMK. In each reaction, $5x10^5$ MKs were incubated with eluates prepared from $7.5x10^6$ patient platelets. MK-bound antibodies were detected using PE-conjugated donkey anti-human IgG and analyzed by flow cytometry. Color-coded numbers indicate the median fluorescence intensity (MFI) of the corresponding peaks. Autoantibodies identified by diagnostic ELISA and by WMK in each patient's platelet eluate are shown above the corresponding flow cytometry plots for comparison. WMK detected weak anti-GPIb/IX autoantibodies in Eluate-1, coexistence of strong anti-GPIIb-IIIa and relatively weak anti-GPIb/IX antibodies in Eluate-2, and strong anti-GPIIb-IIIa antibodies along with an additional uncharacterized antibody in Eluate-3. Further testing with GPIX KO and GPVKO MK was not possible due to the limited availability of patient samples.

## Supplemental methods

### Guide RNA plasmid constructs

gRNAs targeting platelet surface glycoproteins GPIIb, GPIbα, GPIX and GPV were designed using the CRISPR Design Tool https://benchling.com/crispr. gRNA sequences are summarized in *Supplementary Table S2*. Oligos were cloned into the BbsI site of the Cas9 expression plasmids PX459 V2.0 (Addgene).

### Generation of glycoprotein-deficient iPSC lines

B2M KO OT1-1 iPSCs [1] were maintained on Matrigel (Corning)-coated plates in StemFlex Medium (Thermo Fisher Scientific) at 37 °C with 4% $O_2$/5% $CO_2$. The iPSCs were incubated with 10 μM Y27632 for 2 hours before transfection. To generate glycoprotein-deficient iPSC lines, $2x10^5$ cells were transfected with 1 μg of guide plasmid pairs targeting individual gene, including *ITGA2B*, *GPIBA*, *GPIX* or *GPV* using the Amaxa P3 primary cell 4D Nucleofector Kit (Lonza) and Nucleofector Program CB-150. 24-hour post-transfection, 1 μg/ml puromycin was applied for 48 hr. Single clones were harvested at 12 to 14 days post-puromycin-selection and replated on Matrigel-coated plates.

### Generation of IL4Rα-GPIbα iPSC line

T2 guide targeting AAVS1 locus was selected from previous research[2] and cloned into the BbsI site of PX458 plasmids (Addgene). To generate AAVS1 targeting donor plasmid (*Supplementary Figure S5*) for knocking-in transgene encoding IL4Rα-GPIbα chimeric protein, a 1.7 kb gBlock gene fragment (Integrated DNA Technologies) containing AAVS1 homologous arms flanking a splicing acceptor and multiple cloning sites in the middle was first inserted into the XhoI/NotI site of pMiniT 2.0 vector. Three DNA fragments were then assembled into the multiple cloning sites using In-Fusion Snap Assembly EcoDry cloning kit (Takara Bio USA). The 1 kb fragment containing T2A, puromycin resistance gene followed by bovine growth hormone polyadenylation signal was amplified by polymerase chain reaction (PCR) from PX459 V2.0 plasmid. The 3.1 kb human GPIbα promoter cassette was amplified by PCR from pCDNAzeo-hGPIbα pro-hIL4Rα-GPIbα plasmid,[3] a kind gift from Dr. Taisuke Kanaji (The Scripps Research Institute, La Jolla, CA). The 1.4 kb gBlock Gene Fragment encoding IL4Rα-GPIbα fusion protein followed by a rabbit beta-globin polyadenylation signal was synthesize by Integrated DNA Technologies.

To generate IL4Rα-GPIbα iPSC line, $1x10^6$ GPIbα-deficient iPSC were co-transfected with 1 μg of T2 guide plasmid and 3 μg of AAVS1-IL4Rα-GPIbα donor plasmid using the Amaxa P3 primary cell 4D Nucleofector Kit. 48-hour post-transfection 0.5 μg/ml puromycin was applied for 48 hr. Single clones were harvested at 12 to 14 days post-puromycin-selection and replated on Matrigel-coated plates.

### Genotyping

Genomic DNA was extracted from each iPSC clone using the QuickExtract DNA Extraction Solution (Epicenter) following the manufacture's instruction. The regions surrounding the targeted deletion of genes encoding corresponding glycoproteins or the transgene integration site at AAVS1 locus were amplified by PCR using the primers listed in *Supplementary Table S3*. PCR products were analyzed on 1% or 2% agarose gels.

**Differentiation of iPSCs**

CRISPR-edited iPSC lines were differentiated to MK as previously described [4, 5]. Briefly, cells were plated on Matrigel-coated 6-well plates and maintained at 37°C with 4% $O_2$/5% $CO_2$. Media and cytokine changes were followed as described for 9 days except that 1 μM of CHIR99021 (Tocris) was used instead of Wnt3a. Hematopoietic progenitor cells (HPC) in suspension or loosely attached to the bottom were collected by carefully removing the supernatant, then analyzed by flow cytometry to confirm surface expression of CD41 and CD235a. The HPC were further differentiated to MK at 37 °C, 5% $CO_2$ for 6 days in serum-free differentiation medium, a mixture of Iscove's Modified Dulbecco's Medium (Thermo Fisher Scientific) and Ham's F-12 (Corning) at 3:1 ratio, supplemented with 0.5% N2 (Thermo Fisher Scientific), 1% B27 without Vitamin A (Thermo Fisher Scientific), 0.05% BSA (Sigma), 2mM L-glutamine, 50 U/ml penicillin, 50 μg/ml streptomycin, 50 ng/ml SCF and 50 ng/ml TPO (R&D systems). MK were analyzed by flow cytometry to confirm the surface expression of CD41 and CD42b.

**Antigen capture assay**

To locate the epitope targeted by the antibody in patient-17's plasma, $5x10^5$ MK expressing either WT GPIb/IX or IL4Rα-Ib/IX complex were incubated with 50 μl of diluted normal human plasma or ITP patient plasma at room temperature for 1 hour. After three washes with TBS containing 1 mM $CaCl_2$, the cells were solubilized in TBS containing 0.1 mM $CaCl_2$, 1% Triton X-100 and protease inhibitor cocktail. After removing insoluble material by centrifugation at 20,000g for 30 minutes, the cell lysates were applied to a well of 96-well microplate that contains fixed mAb against either GPIbα (142.17) or IL-4Rα (25463). After 1 hour incubation, the plate was washed four times with TBS containing 0.1 mM $CaCl_2$, 0.1% Tween 20, and 3% BSA. Well-bound human antibodies were detected with horseradish peroxidase-conjugated donkey anti-human IgG and ultra TMB ELISA substrate solution. The reaction was stopped by addition of sulfuric acid, and the optical density (OD) was measured at 450 nm.

References

1. Zhang N, Santoso S, Aster RH, Curtis BR, Newman PJ. Bioengineered iPSC-derived megakaryocytes for the detection of platelet-specific patient alloantibodies. Blood. 2019;134(22):e1-e8.
2. Mali P, Yang L, Esvelt KM, et al. RNA-guided human genome engineering via Cas9. Science. 2013;339(6121):823-826.
3. Kanaji T, Russell S, Ware J. Amelioration of the macrothrombocytopenia associated with the murine Bernard-Soulier syndrome. Blood. 2002;100(6):2102-2107.
4. Mills JA, Paluru P, Weiss MJ, Gadue P, French DL. Hematopoietic differentiation of pluripotent stem cells in culture. In: Qu KDBaC-K, ed. Methods in Molecular Biology. New York: Springer Science+Business Media, 2014:181-194.
5. Paluru P, Hudock KM, Cheng X, et al. The negative impact of Wnt signaling on megakaryocyte and primitive erythroid progenitors derived from human embryonic stem cells. Stem cell research. 2014;12(2):441-451.